Applied Physics A (2019) 125:559
https://doi.org/10.1007/s00339-019-2849-5

Applied Physics A
Materials Science & Processing

A comparative study on the color change of pigments due to the consolidation of conventional spectroscopic techniques and laser-induced breakdown spectroscopy

Ayman Mohamed Mostafa[1] · Safa Abd El-Kader Mohamed Hamed[2] · Hala Afifi[2] · Samia Mohamady[3]

Received: 25 April 2019 / Accepted: 29 June 2019 / Published online: 25 July 2019

Abstract
The present study seeks to investigate the changes in the elemental composition of pigments due to consolidation. Therefore, the effect of the consolidation of hydroxypropyl cellulose (Klucel G) of different concentrations and its mixture with zinc oxide (ZnO) nanoparticles on the black, red, and ochre pigments applied on chalk-based preparation layers before and after aging were studied. Additionally, the role of ZnO nanoparticles in protecting the pigments after UV aging has been examined. The color change due to consolidation solutions was measured by the spectrophotometer, scanning electron microscopy with energy dispersive X-ray (SEM–EDX), and laser-induced breakdown spectroscopy (LIBS). Interestingly, the results revealed that all the painted samples treated with Klucel G (1%) and nano-ZnO (1%), as additives, showed the least color change values. Moreover, SEM–EDX and LIBS analyses prove the ability of ZnO nanoparticles to enhance the durability of consolidants and coatings toward aging.

1 Introduction

Pigments were widely used in Ancient Egypt. They mainly consisted of naturally occurring minerals. Tests performed on polychromy artefacts revealed the materials that were traditionally employed in the different pigments [1, 2]. It is known that pigments are subjected to color change phenomenon due to artificial and natural aging. Light plays a significant role in the degradation of the pigments notably ultraviolet irradiation of wavelengths 225–350 nm [3]. Moreover, polychrome objects are subjected to interior factors such as the loss of the objects' structural resistance, as well as exterior factors, e.g. the environmental conditions, biological activity, and pollution. They are often acting in synergy. Another factor to consider is the conservation interventions on the objects, especially cleaning and consolidation, which might affect the stability of pigments in the paint layers [4, 5].

The major problem of pigment degradation are fading, altering the legibility of the polychrome objects, and causing flaking or powdering of paint layers. To preserve the coherence of the polychrome objects and the paint layer in many cases, objects are consolidated with different adhesives. However, most of the studies have addressed the consolidation painting objects, sought new materials and developing micro and nanocomposites, and neglected their effect on the pigments themselves, especially after aging [6–10].

Different analytical techniques, including the polarized light microscopy (PLM), (SEM–EDX), and laser-induced fluorescence (LIF), have been employed to examine the painted layers in the pigments and investigate the fundamentals of the objects (i.e., morphology, optical, phase, and elemental analysis). To be applied to the cultural heritage, these techniques should have a minimal destructive ability [11–16].

Thus, effective tools for pigment identification and assessment should always be sought and developed. The LIBS has attracted considerable attention recently from the researchers of archaeology to collect more information about the studied samples [17, 18]. Moreover, it does not require any complicated preparation of the sample and the dose. It is also not destructive on the surface of the sample. Using this

✉ Safa Abd El-Kader Mohamed Hamed
safa_an78@yahoo.com; safa_hamed@cu.edu.eg

[1] Laser Technology Unit, Center of excellent for advanced science, National Research Centre, 33 El Bohouth st. (former El Tahrir st.), Dokki, Giza 12622, Egypt

[2] Conservation Department, Faculty of Archaeology, Cairo University, Giza 12613, Egypt

[3] Ministry of Antiquities, Cairo, Egypt

technique, we could detect the multi-elements, especially the light ones in a short time and by using the micro dimension of the sample [19]. This process is produced by collecting the emitted plasma light from the ablated laser interacting with the surface of the matter. Moreover, the ablation that happens in the microscale dimension, leads to ejecting very tiny particles, ions, and clusters formed by the body of the plasma [20, 21]. Recently, archaeologists have used LIBS to analyze prehistoric paintings on the walls, to distinguish the pigment from the wall matrix, especially when the samples show very irregular surface, and to identify the superimposed layers and composition [22–25].

Since the characterization of materials in archaeological artefacts helps preserve them significantly, different techniques, chemical and physical, can be used to detect the changes in the elemental composition of the pigments. Thus, the SEM–EDX micro-analysis, UV–visible spectrometer, and LIBS are utilized and compared to examine the preparation procedures and conservation processes, especially consolidation, of the painted objects of three natural mineral pigments (black, red, and yellow). The effect of adding ZnO nanoparticles to the consolidants is also studied.

2 Materials and method

2.1 Painted samples

Three natural minerals, namely black (carbon), red (hematite) and yellow ochre (iron oxides), were selected as pigments. Then, they were immersed in water that was changed daily for 7 days to leach out the salts and impurities. After that, previously seasoned sycamore samples measured ($10 \times 10 \times 2$ cm) were covered with preparation layers of chalk and calcium carbonate ($CaCO_3$) and mixed with a previously prepared animal glue solution (1 glue:15 water v/v). The chosen pigments were mixed with the same solution of the animal glue to prepare the paints that were applied to the chalk-based preparation layers (six samples used for each paint sample).

2.2 Consolidation solutions

An adhesive was chosen as a consolidant; (Klucel G) and ZnO nanoparticles. The Klucel G was supplied by CTS imported by Andalus Company for Conservation and Restoration supplies. Concentrations 1%, 2% and 3% of Klucel G in ethyl alcohol 95% were selected to use. The ZnO nanoparticles powder (supplier: Sigma & Aldrich) was added to Klucel G solution 1% at ratios of 1 wt% based on the weight of dry Klucel G. The solutions were homogenized using a high shear homogenizer at 10,000 rpm (CAT high-speed homogenizer. Gmbh).

2.3 Application of consolidants

The prepared consolidation solutions were applied to the painted samples by brushing at room temperature. Following consolidation, the pigmented samples were left to dry. Then, they were aged by subjecting the untreated and treated pigment samples for UV aging using mercury lamp for 50 h to UVA (5.5616 mW/cm^2) and UVC (3.0782 mW/cm^2) at a stable temperature of 25.5 ± 1 °C and relative humidity 32 ± 4% at the National Institute of Standards (NIS) in Giza, Egypt. Finally, all samples were examined.

2.4 Characterization techniques

2.4.1 Measurement of color change by the spectrophotometer

The color changes are measured by a Hunterlab colorimeter. Applying the CIELAB color system, the color parameters L^*, a^*, and b^* as well as the overall change in color indices (ΔE^*) are determined in each sample before and after consolidation and aging. The total color changes (ΔE^*) due to consolidation treatment, are calculated based on the following equation [26]:

$$\Delta E = \sqrt{(\Delta L^*)^2 + (\Delta a^*)^2 + (\Delta b^*)^2},$$

where ΔL^*, Δa^* and Δb^* are the changes of the color coordinates L^*, a^* and b^* for the treated aged samples, compared to the control (untreated) sample.

2.4.2 SEM–EDX microanalysis

The SEM is carried out using a Philips XL 30 scanning microscope equipped with EDX Ametek Octane Pro microanalytical system. The spot analysis is carried out using an accelerating voltage of 20 kV, a working distance of 10 mm, a magnification of 500×, and a scanning time of 1 min. For pigment identification, the elemental composition of the black, red, and yellow ochre pigments is identified before and after the application on the chalk-based preparation layers. The samples painted with these pigments are analyzed before and after consolidation and aging. Moreover, four spots for each pigment are analyzed to obtain the mean values.

2.4.3 LIBS

In the LIBS experimental setup, the nanosecond infrared laser of Nd:YAG (PL9000, Continuum laser, made in the USA) produces a laser beam with a diameter of 0.5 ± 0.1 mm, energy of 100 mJ/pulse, a repetition rate of 10 Hz, and a fundamental wavelength of 1064 nm. This laser

radiation is focused by a plano-convex quartz lens with a focal length up to 70 mm. It is directed to the surface of the sample that is mounted on a holder, connected to the *X–Y–Z* motorized stage, and performed at the atmospheric pressure. Once the focusing laser irradiation interacts with the surface of the sample, the plasma plume is produced and the emitted light is obtained. It is collected and transferred using fiber-optics with a diameter of 0.6 mm and a length of 50 cm of Czerny-Turner spectrometer (Acton SP2500i, made in USA). The used dispersion grating has 2400 lines/mm and scans the wavelength from 200 to 900 nm based on the linear dispersion with a resolution of 0.05 nm. The monochromator is coupled with an intensified charge-coupled device (ICCD camera, PI MAX, 1KRB-FG-43, gating time < 2 ns). Data acquisition and spectroscopic analysis are performed using WinSpec/32 software, LIBS++ software and appropriate database (open tools for analyzing the LIBS).

2.4.4 Statistical analysis

The elemental composition of the black, red and yellow ochre pigments is analyzed using SPSS (version 22, IBM, Inc.). The group comparison of all samples is done using repeated measures of the analysis of variance (ANOVA) to detect the overall differences between the means of the outcome measures. For all measures, the significance is set at an alpha level of 0.05 and the data are presented as means and standard deviations (SDs).

3 Result and discussion

3.1 Identification of pigments

3.1.1 SEM–EDX microanalysis

The elemental composition of the black, red, and yellow ochre pigments was identified by the measurements of the SEM/EDX analysis. This technique helps provide elemental analysis as semi-qualitative and semi-quantitative information of the measured samples, used to understand their molecular structure. It is based on generating the X-ray radiation in atoms of the measured samples, followed by a set of physical events inside the atoms, where the irradiated atoms are ionized and emit the X-ray radiation of this element. Finally, the sensitive detector is used to collect the emitted wavelengths based on the element's atomic number. The results are shown in Table 1, illustrating that black is composed mainly of C, O, Ca, S, and P. Red is composed of Fe, O, Al, and Si, while Yellow ochre is composed of Fe, O, Al, Si, P, S, K, and Ti. Thus, it is concluded that applying the three pigments on chalk-based preparation layers shows other elements described as; The appearance of C and K in red and yellow; N in black and red; Si and Cl in black; Ti, S, and P in red; Na in the three pigments; Mg in the three pigments due to their presence in these preparation layers. These elements can be represented as the main elements of these colored pigments.

Table 1 The elemental analysis [qualitative and semi quantitative (atomic weight percentage)] of black, red and ochre paints"

Elements	Black (%)	Red (%)	Yellow (%)
C	53.87 ± 14.28	–	–
O	31.51 ± 9.75	35.18 ± 4.89	57.51 ± 1.89
Al	–	1.59 ± 1.38	2.54 ± 0.19
Si	–	7.77 ± 0.32	5.20 ± 1.44
P	0.02 ± 0.05	–	0.17 ± 0.29
S	0.47 ± 0.14	–	0.89 ± 0.02
K	–	–	0.38 ± 0.01
Ti	–	–	0.63 ± 0.02
Fe	–	55.37 ± 5.65	32.66 ± 2.63
Ca	14.13 ± 4.72	–	–

3.1.2 LIBS

Most of the materials have a complex molecular structure with multi-elements. These elements can differ in the phase, ratio, number, etc. Additionally, atomic and molecular spectroscopy is used to illustrate this complex situation. Therefore, LIBS is utilized to give a lot of information and understand the molecular structure [27]. It is based on making laser-matter interaction with the surface of the measured sample to produce plasma plume with high pressure and adequate temperature to ionize and vaporize most of the periodic table. This ionization process excites the atoms to the higher electronic levels, followed by the relaxation step before returning to steady state and emitting spectral lines at specific wavelengths for each element. The emitted wavelengths in the plasma are collected by a lens and transferred to spectrograph by a fiber optic to be dispersed using different grating. The dispersed lines are detected by the detector and collected by a spectrum. The LIBS spectra of the colored pigment of black, orange, and yellow recorded after the post-laser shots in a different spectral region are presented in Fig. 1a–c. Each LIBS spectrum is collected after measuring five single shots spectra acquired in different points of the sample surface. The spectral range chosen is 200–900 nm due to the presence of the most abundant emission lines of pigment elements. The LIBS analysis of the samples reveals the presence of C, O, P, Ca, Na, Mg, and Si as the main constituents in different percentages. Moreover, special elements characterize each color. In the black pigment, there are Ti and Al. In the red pigment, there are

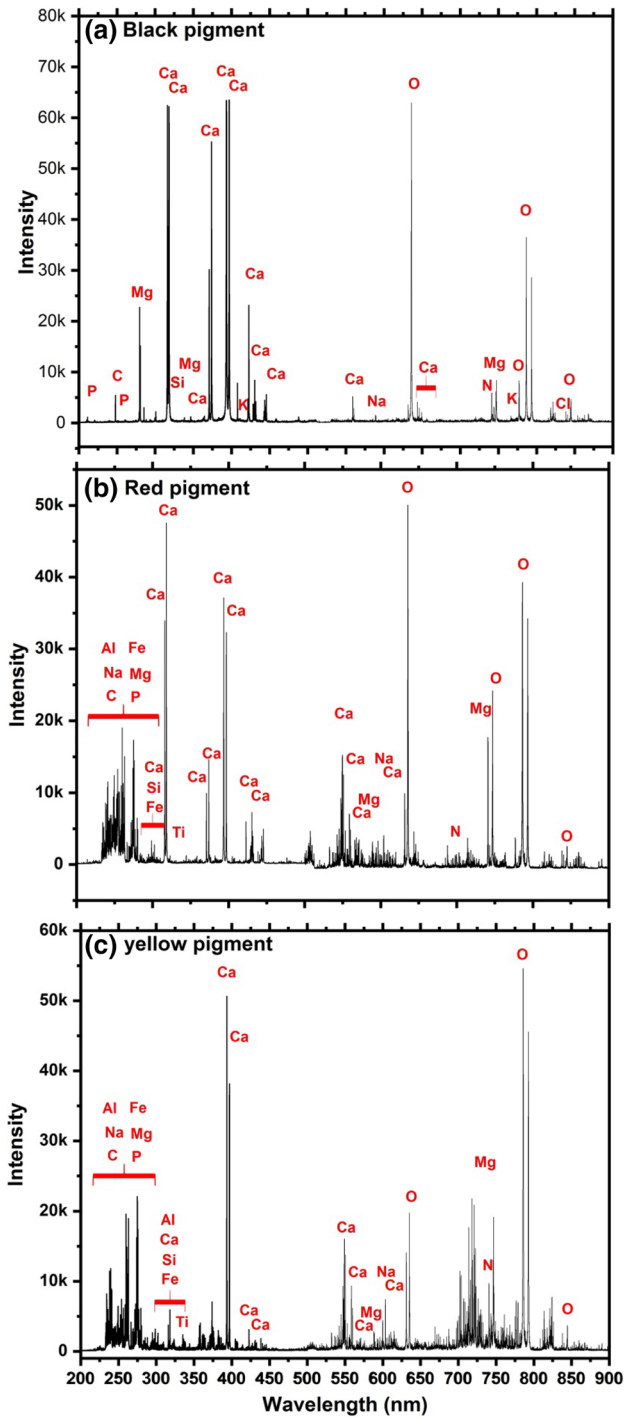

Fig. 1 LIBS spectra acquired on the surface of **a** black, **b** red, and **c** yellow pigment

Fe, Al, and Si. In the yellow color, there are Fe, Al, Si, and Ti [28, 29].

In Fig. 1a–c, the most intense features originate from the excited Ca ions at 317.76 nm and 319.55 nm [30]. These emissions of spectral lines strongly appear in all pigment samples, suggesting the abundance of Ca. When absorbing water, the Ca hydroxide form is produced on the surface of the dry plaster of the pigment and interacts with the atmospheric CO_2. These interactions help prepare a thin top Ca layer used as a locker of the function group of pigment from the environmental deposits (pollution and/or bird excrements) [31]. In addition, the LIBS spectra show intense emission bands of C, O, P, Na, and Mg in the chemical structure of the colored pigments. In Fig. 1a, the analysis of the colored red pigment reveals that the spectrum contains impurities from P element. Moreover, the detection of C indicates the presence of organic oil form in the hydrocarbon structure (C, H, and O) [32].

In Fig. 1b, the analysis of the colored red pigment reveals that the spectra are richer in Fe spectral lines of Fe than other pigments [33]. Based on the large atomic and ionic number of Fe emission lines, the crowded spectral lines give rise to a quite complex spectrum with overlapping and often inadequately resolved features. However, the presence of iron could be investigated by the main characteristic peaks obtained from pure iron-based pigments [34]. In the presence of O and Si, this increase is related to the presence of a high amount of iron oxides and aluminum-silicates as main constitutes of the red pigments. Moreover, the pigment still contains Ca, demonstrating the presence of the lime impurities in the red painting structure. This investigation proves the identification of red as an inorganic iron-based pigment constituted by hematite [35]. In Fig. 1c, the high amount of Fe in this pigment makes the spectrum too crowded with a large number of its spectral lines, which affect the clear appearance of other spectral lines of P, Na, C, and Al.

3.2 Studying the effect of consolidation on the pigments

3.2.1 Measurement of color change by spectrophotometer

Table 2 shows the values of changes in the color (ΔE) for the chosen paint samples after consolidation and UV aging. The results of the red samples indicate a slight difference in the consolidated samples with Klucel G compared to the reference one (sample 1). While this difference rises by increasing Klucel G concentration in samples 2, 3, and 4 (by 1%, 2%, and 3%, respectively), it is rated the lowest in sample 5 (treated with Klucel G 1% and nano-ZnO 1% as additives). The black samples show a dramatic increase in ΔE because of the consolidation treatment and aging. Expectedly, the higher Klucel G concentration is, the more the color change values become, as shown in samples 7, 8 and 9 (treated with Klucel G by 1%, 2%, and 3%, respectively). Like the red samples, the ΔE reduces in sample 10 (treated with Klucel G 1% and nano-ZnO 1% as additives). The results of the yellow ochre samples are almost the same as those detected in the black samples.

Table 2 The changes in the color values for the paint samples after treatment and aging

Sample no.	Paint	Treatment	ΔL	Δa	Δb	ΔE
1	Red	Reference sample	1.13	0.34	0.24	1.20
2		Klucel G 1%	1.16	0.54	− 0.51	1.38
3		Klucel G 2%	1.51	0.21	− 0.42	1.58
4		Klucel G 3%	1.56	0.46	− 0.11	1.63
5		Klucel G 1% + nano-ZnO 1%	1.15	0.50	− 0.49	1.33
6	Black	Reference sample	2.44	0.16	0.00	2.45
7		Klucel G 1%	3.07	0.16	0.30	3.09
8		Klucel G 2%	3.21	0.14	0.45	3.24
9		Klucel G 3%	4.05	0.18	0.13	4.06
10		Klucel G 1% + nano-ZnO 1%	2.84	0.16	0.15	2.85
11	Ochre	Reference sample	1.07	− 0.23	0.10	1.10
12		Klucel G 1%	1.54	− 1.00	0.57	1.92
13		Klucel G 2%	2.73	− 1.35	0.81	3.15
14		Klucel G 3%	3.48	− 1.15	1.48	3.95
15		Klucel G 1% + nano-ZnO 1%	1.60	− 1.20	0.50	2.06

Moreover, the highest ΔE values are apparent in samples 12, 13 and 14 (treated with Klucel G by 1%, 2%, and 3%, respectively). However, these changes decrease in sample 15 (treated with Klucel G 1% and nano-ZnO 1% as additives).

Table 2 shows that the red paint represents the lowest color change values as a result of consolidation and aging. Notably, the ΔE values of the samples painted with black and yellow ochre, consolidated with KlucelG, and aged are higher than the ΔE values of the samples painted with red. This may be caused by sulphur found in black and yellow ochre composition only (Table 1). Interestingly, all the painted samples treated with Klucel G 1% and nano-ZnO 1% as additives show the least color change values because nano-ZnO protect the pigments against UV effects [36, 37]. Accordingly, the painted samples treated with Klucel G (2% and 3%) are excluded from the rest of the investigations because they increase the color change of pigments.

3.2.2 SEM–EDX microanalysis

Table 3 shows the increasing percentage of C, as the main element in black paint, after aging. This percentage decreases in the sample treated with Klucel G 1%. However, the sample treated with Klucel G 1% and nano-ZnO 1% shows the highest percentage of C.

The red samples reveal the high concentration of Fe and O, as the main elements, after consolidation and aging (Table 4). The sample treated with Klucel G 1% and nano-ZnO 1%, as additives achieve the highest percentage of Fe. Moreover, the yellow ochre samples show almost the same results as the red ones (Table 5). The overall results indicate that UV aging affects some elements in the chalk-based preparation layers, which increases the concentration of the main elements of the three paints; black, red and yellow ochre. Surprisingly, the percentage of the main elements in the three paints reduces in the samples consolidated with

Table 3 The elemental analysis [qualitative and semi quantitative (atomic weight percentage)] of samples painted with black before and after consolidation and aging

Elements	Before aging (%)	After aging (%)	Klucel G 1 and after aging (%)	Klucel G1 + nano-ZnO and after aging (%)
C	24.61 ± 0.83	50.51 ± 0.58	20.17 ± 1.34	51.06 ± 2.12
N	–	14.44 ± 0.87	3.66 ± 0.58	13.14 ± 0.99
O	47.53 ± 1.99	20.44 ± 0.78	46.52 ± − 0.39	21.88 ± 1.31
Na	–	0.70 ± 0.09	0.67 ± 0.07	1.05 ± 0.06
Mg	0.36 ± 0.08	0.54 ± 0.06	0.61 ± 0.07	0.48 ± 0.04
Al	–	0.36 ± 0.08	0.42 ± 0.03	0.25 ± 0.04
Si	–	0.32 ± 0.12	0.69 ± 0.09	0.32 ± 0.07
S	1.6400 ± 0.44	1.08 ± 0.16	1.36 ± 0.25	1.83 ± 0.09
Cl	–	0.45 ± 0.06	0.28 ± 0.02	0.58 ± 0.04
Ca	26.22 ± 0.73	11.17 ± 0.78	25.63 ± 1.26	9.12 ± 0.52

Table 4 The elemental analysis [qualitative and semi quantitative (atomic weight percentage)] of samples painted with red before and after consolidation and aging

Elements	Before aging (%)	After aging (%)	Klucel G 1 and after aging (%)	Klucel G1 + nano-ZnO and after aging (%)
C	50.07 ± 6.84	10.24 ± 2.40	17.17 ± 1.34	11.21 ± 1.01
N	9.77 ± 1.74	–	–	–
O	23.03 ± 3.64	41.46 ± 1.29	41.42 ± 1.54	39.08 ± 0.03
Na	0.91 ± 0.11	1.34 ± 0.40	0.61 ± 0.71	1.53 ± 0.47
Mg	–	0.96 ± 0.18	0.89 ± 0.26	1.04 ± 0.58
Al	0.79 ± 0.37	2.20 ± 0.13	1.88 ± 0.48	1.94 ± 0.40
Si	2.14 ± 1.20	9.0 ± 3.04	6.63 ± 1.42	8.93 ± 3.80
P	0.83 ± 0.13	0.37 ± 0.09	0.26 ± 0.12	0.34 ± 0.35
S	0.49 ± 0.14	1.63 ± 0.47	3.30 ± 0.23	1.51 ± 0.40
K	0.25 ± 0.05	0.55 ± 0.04	0.62 ± 0.07	0.57 ± 0.13
Ca	2.14 ± 0.47	2.85 ± 0.17	6.93 ± 0.69	3.39 ± 0.01
Ti	–	0.18 ± 0.1	0.13 ± 0.05	0.24 ± 0.19
Fe	9.59 ± 2.81	29.24 ± 1.25	19.07 ± 1.92	30.28 ± 0.25

Table 5 The elemental analysis [qualitative and semi quantitative (atomic weight percentage)] of samples painted with yellow ochre before and after consolidation and aging

Elements	Before aging (%)	After aging (%)	Klucel G 1 and after aging (%)	Klucel G1 + nano-ZnO and after aging (%)
C	57.23 ± 4.82	10.52 ± 1.34	19.48 ± 1.86	8.83 ± 0.72
O	25.75 ± 2.62	49.74 ± 1.30	50.16 ± 1.85	50.07 ± 2.41
Na	0.61 ± 0.06	1.63 ± 0.38	–	–
Mg	0.49 ± 0.11	0.56 ± 0.23	–	–
Al	0.58 ± 0.09	1.48 ± 0.08	1.60 ± 0.37	1.90 ± 0.26
Si	1.05 ± 0.17	2.64 ± 0.28	2.81 ± 0.65	3.31 ± 0.35
P	–	0.69 ± 0.02	0.52 ± 0.22	0.74 ± 0.14
S	1.52 ± 0.34	3.45 ± 0.15	2.26 ± 0.54	2.78 ± 0.20
K	0.46 ± 0.02	0.56 ± 0.07	0.52 ± 0.11	0.76 ± 0.21
Ca	3.78 ± 1.35	7.05 ± 0.92	4.89 ± 1.33	4.59 ± 0.95
Ti	0.19 ± 0.01	0.40 ± 0.02	0.38 ± 0.07	0.49 ± 0.13
Fe	7.56 ± 0.89	21.31 ± 1.27	17.38 ± 0.92	26.54 ± 3.10

Klucel G 1% because all cellulose ethers experience chain breaking due to oxidation enhanced by light exposure [38, 39]. Furthermore, the percentage of the main elements of the three paints increases in the samples consolidated with Klucel G 1% and nano-ZnO 1% as additives due to the ability of ZnO nanoparticles to enhance the durability of consolidants and coatings towards UV aging [37, 40, 41].

3.2.3 LIBS

The effect of consolidation and UV aging on the surface of the pigments is also explored using LIBS based on identifying the pigment concentration in each case study. The concentration is detected, focusing on the main element in each pigment. Clearly, C represents the main element in the black pigment at a spectral line of 247.8 nm [42], while the Fe element represents the most abundant element in the red and yellow pigments at spectral lines of 259.98, 261.25, and 263.18 nm [43]. Thus, the effect of consolidation treatment and UV aging on the surface of used pigment are detected by defining their amount of C or Fe after the correlation of the whole LIBS spectra. The correlation process is done by a normalization process to assert that the intensity of the whole spectra in each measurement has not changes because of the sample holder or another factor. The normalization process is done by dividing the whole spectra by the hydrogen peak line (H alpha) at a value of 658 nm [44]. Figure 2 illustrates that C and Fe are the main elements in the black and red/yellow pigments, respectively. It also indicates that the spectrum is corrected by a normalization process to detect any change in the concentration through investigating the intensity of their elements (C and Fe). Obviously,

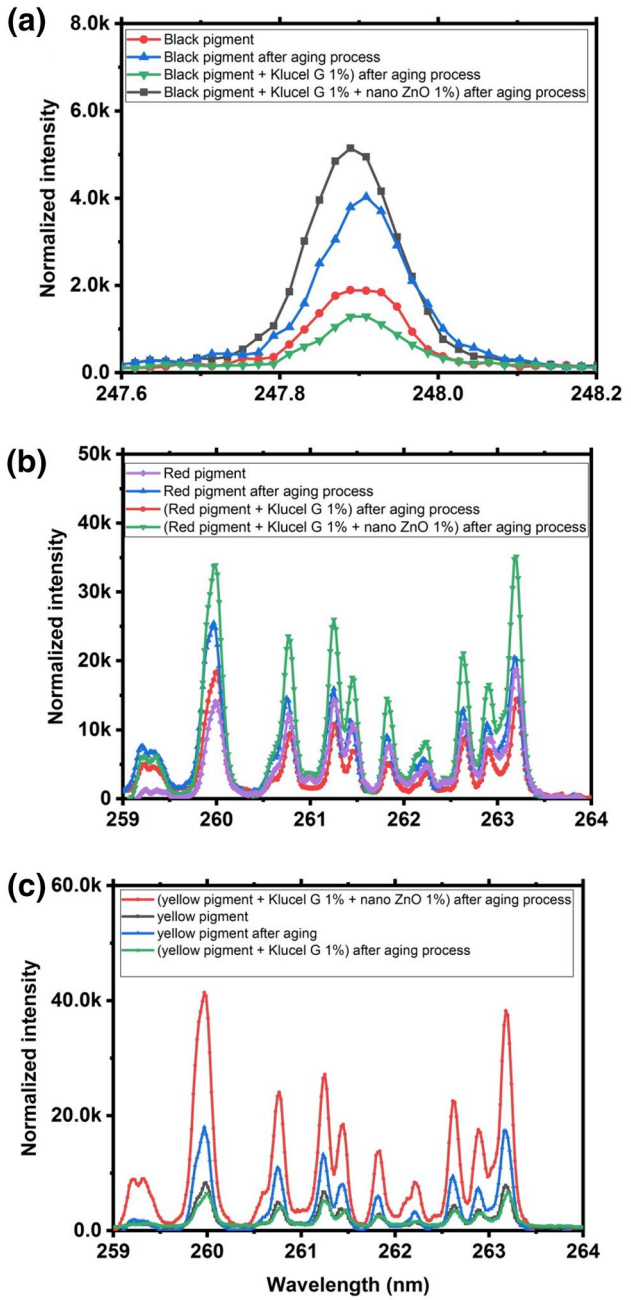

Fig. 2 LIBS normalized spectra of the effect of aging process without any additive and with the additive of klucel G 1% and klucel G 1% + nano ZnO 1% on the surface of **a** black, **b** red, and **c** yellow pigment

the amounts of C (in case of black pigment) and Fe (in case of red/yellow pigment) change when the intensity changes after UV aging. Their intensity increases with no consolidation treatment and decreases if consolidated with Klucel G. Moreover, significant increases are observed in the case of the consolidation with Klucel G and the addition of nano-ZnO. The above-mentioned results are compatible with the results of SEM–EDX.

4 Conclusion

The investigations of pigments carried out by SEM–EDX and LIBS helped identify the elemental composition of the black, red and yellow pigments before and after the application on a chalk-based layer. Thus, the results obtained from the LIBS and SEM–EDX were identical in investigating the elements of each colored pigment. The effect of nano-ZnO on protecting the colored pigments was also investigated. Based on SEM–EDX, the percentage of the main elements of the three paints increased in the samples consolidated with Klucel G 1% and nano-ZnO 1% as additives because of the ability of nano-ZnO to enhance the durability of consolidants and coatings towards UV aging. The LIBS revealed that the intensity of the main elements of the pigments increased in the case of consolidation with KlucelG and the addition of nano-ZnO. Hence, the results of the LIBS and SEM–EDX were identical in defining the elements of the pigments. This shows the role of nano-ZnO in protecting the pigments from UV effects, which enhance the durability of the consolidants and coatings towards aging. Further studies are required to explore other changes in pigments due to various materials are used in the treatment of archaeological objects.

References

1. S. Colinart, S. Pages-Camagna, *Egyptian Polychromy: Pigments of the "Pharaonic Palette"*, ed. by W. Yongqi, Z. Tinghao, M. Petzet, E. Emmerling, C. Blansdorf. The Polychromy of Antique Sculptures and the Terracotta Army of the First Chinese Emperor: Studies on Materials, Painting Techniques and Conservation. International conference in Xi'an, Shaanxi History Museum, March 22–28, 1999, Munich 2001, p. 85–88. https://doi.org/10.11588/monstites.2001.0.22337
2. Marti AP. Spectroscopic Analytical Methodologies for the Study of Cultural Heritage Materials. PhD, Faculty of Science, Autonomous University of Barcelona (2011). https://ddd.uab.cat/pub/tesis/2014/hdl_10803_285774/apm1de1.pdf
3. T. Ishitani, K. Umeda, S. Kimura, Studies on the degradation of natural pigments, Part 1. Photodegradation of lycopene and *B*-carotene. Nippon Shokuhin Kogyo Gakkaishi **23**(10), 480–485 (1976). https://www.jstage.jst.go.jp/article/nskkk1962/23/10/23_10_480/_pdf/-char/en
4. M. Munteanu, I. Sandu, V. Vasilache, I.C.A. Sandu, Disadvantages of using some polymers in restoration of old icons on wooden panels. Int. J. Conserv. Sci. **7**(1), 349–356 (2016). http://www.ijcs.uaic.ro/public/IJCS-16-SI17_Munteanu.pdf
5. A. Coccato, L. Moens, P. Vandenabeele, On the stability of mediaeval inorganic pigments: a literature review of the effect of climate, material selection, biological activity, analysis and conservation treatments. Herit. Sci. **2017**, 5–12 (2017). https://doi.org/10.1186/s40494-017-0125-6
6. M.D. Gayo, E. Parra, A. Carrassón, Technical examination and consolidation of the paint layers on a mudéjar coffered ceiling

in the Convent of Santa Fe, Toledo. Stud. Conserv. **37**(1), 54–56 (2013). https://doi.org/10.1179/sic.1992.37.1.54
7. G.A. Berger, Testing adhesives for the consolidation of painting. Stud. Conserv. **17**(4), 173–194 (1972). https://doi.org/10.1179/sic.1972.016
8. K. Catenazzi, Evaluation of the use of Funori for consolidation of powdering paint layers in wall paintings. Stud. Conserv. **62**(2), 96–103 (2017). https://doi.org/10.1080/00393630.2015.1131043
9. S.A.M. Hamed, Possibilities application of nanoscience and nanotechnology in conservation of archaeological wood: a review. Jokull J. **63**(12), 9–19 (2013)
10. P. Baglioni, E. Carretti, D. Chelazzi, Nanomaterials in art conservation. Nat. Nanotechnol. **10**, 287–290 (2015). https://www.researchgate.net/publication/274726417_Nanomaterials_in_art_conservation
11. V. Perdikatsis, H. Brecoulaki, The Use of Red and Yellow Ochres as Painting Materials in Ancient Macedonia, in *Proceedings of the 4th Symposium of the Hellenic Society for Archaeometry, National Hellenic Research Foundation, Athens, 28-31 May 2003, BAR International Series 1746*, ed. by Y. Facorellis, N. Zacharias, K. Polikreti (BAR International Series, Athens, 2008), pp. 559–567. https://www.academia.edu/2776893/The_Use_of_Red_and_Yellow_Ochres_as_Painting_Materials_in_Ancient_Macedonia
12. M. Uda, Characterization of Pigments Used in Ancient Egypt, in *X-Rays for Archaeology*, ed. by M. Uda, G. Demortier, I. Nakai (Springer, Berlin, 2005), pp. 3–26. https://doi.org/10.1007/1-4020-3581-0_1
13. D. Lau, P. Kappen, M. Strohschnieder, N. Brack, P.J. Pigram, Characterization of green copper phase pigments in Egyptian artifacts with X-ray absorption spectroscopy and principal components analysis. Spectrochim. Acta Part B **63**, 1283–1289 (2008). https://www.sciencedirect.com/science/article/abs/pii/S058485470800270X
14. R. Siddall, Mineral pigments in archaeology: their analysis and the range of available materials. Minerals **8**(201), 1–35 (2018). https://www.mdpi.com/2075-163X/8/5/201
15. O. Ionescu, D. Mohanu, A. Stoica, G. Baiulescu, Analytical contributions to the evaluation of painting authenticity from Princely church of Curtea de Arges. Talanta **63**(4), 815–823 (2004)
16. A. Braz, M. López-López, C. García-Ruiz, Raman spectroscopy for forensic analysis of inks in questioned documents. Forensic Sci. Int. **232**(1–3), 206–212 (2013). https://www.sciencedirect.com/science/article/pii/S037907381300368X
17. A. Giakoumaki, K. Melessanaki, D. Anglos, Laser-induced breakdown spectroscopy (LIBS) in archaeological science—applications and prospects. Anal. Bioanal. Chem. **387**, 749–760 (2007). https://doi.org/10.1007/s00216-006-0908-1
18. J. Anzano, J. Gutierrez, M. Villoria, Direct determination of aluminum in archaeological clays by laser-induced breakdown spectroscopy. Anal. Lett. **38**, 1957–1965 (2005). https://www.researchgate.net/publication/233221336_Direct_Determination_of_Aluminum_in_Archaeological_Clays_by_Laser-Induced_Breakdown_Spectroscopy
19. M.M. ElFaham, M. Okil, A.M. Mostafa, Limit of detection and hardness evaluation of some steel alloys utilizing optical emission spectroscopic techniques. Opt. Laser Technol. **108**, 634–641 (2018). https://www.sciencedirect.com/science/article/pii/S0030399218309976
20. A.M. Mostafa, M.F. Hameed, S.S. Obayya, Effect of laser shock peening on the hardness of AL-7075 alloy. J. King Saud Univ. Sci. (2017). https://www.researchgate.net/publication/318935718_Effect_of_Laser_Shock_Peening_on_the_Hardness_of_AL-7075_Alloy
21. R. Noll, *Laser-Induced Breakdown Spectroscopy* (Springer, Berlin, 2012), pp. 7–15
22. A. Brysbaert, K. Melessanaki, D. Anglos, Pigment analysis in Bronze Age Aegean and Eastern Mediterranean painted plaster by laser-induced breakdown spectroscopy (LIBS). J. Archaeol. Sci. **33**(8), 1095–1104 (2006)
23. P. Singh, E. Mal, A. Khare, S. Sharma, A study of archaeological pottery of Northeast India using laser induced breakdown spectroscopy (LIBS). J. Cult. Herit. **33**, 71–82 (2018). https://www.sciencedirect.com/science/article/abs/pii/S1296207417304399
24. V. Tankova, G. Malcheva, K. Blagoev, L. Leshtakov, Investigation of archaeological metal artefacts by laser-induced breakdown spectroscopy (LIBS). J. Phys. Conf. Ser. IOP Publ. **2018**, 012003 (2018). https://doi.org/10.1088/1742-6596/992/1/012003/pdf
25. A. Botto, B. Campanella, S. Legnaioli, M. Lezzerini, G. Lorenzetti, S. Pagnotta et al., Applications of laser-induced breakdown spectroscopy in cultural heritage and archaeology: a critical review. J. Anal. Atom. Spectrom. **34**, 81–103 (2019). https://pubs.rsc.org/en/content/articlelanding/2019/ja/c8ja00319j#!divAbstract
26. W. George, *Hand Book of Material Weathering*, 2nd edn. (Chem Tec, Ontario, 1995)
27. Á. Fernández-Bravo, T. Delgado, P. Lucena, J.J. Laserna, Vibrational emission analysis of the CN molecules in laser-induced breakdown spectroscopy of organic compounds. Spectrochim. Acta Part B Atom. Spectrosc. **89**, 77–83 (2013). https://kundoc.com/pdf-vibrational-emission-analysis-of-the-cn-molecules-in-laser-induced-breakdown-spe.html
28. D. Anglos, S. Couris, C. Fotakis, Laser diagnostics of painted artworks: laser-induced breakdown spectroscopy in pigment identification. Appl. Spectrosc. **51**, 1025–1030 (1997). https://doi.org/10.1366/0003702971941421
29. M. Mateo, T. Ctvrtnickova, G. Nicolas, Characterization of pigments used in painting by means of laser-induced plasma and attenuated total reflectance FTIR spectroscopy. Appl. Surf. Sci. **255**(10), 5172–5176 (2009). https://www.researchgate.net/publication/223817079_Characterization_of_pigments_used_in_painting_by_means_of_laser-induced_plasma_and_attenuated_total_reflectance_FTIR_spectroscopy
30. D. Body, B. Chadwick, Optimization of the spectral data processing in a LIBS simultaneous elemental analysis system. Spectrochim. Acta Part B Atom. Spectrosc. **56**(6), 725–736 (2001). https://www.sciencedirect.com/science/article/abs/pii/S0584854701001860
31. H. Hotokezaka, N. Aoyagi, Y. Kawahara, N.U. Yamaguchi, S. Nagasaki, K. Sasaki et al., Selective and in situ determination of carbonate and oxide particles in aqueous solution using laser-induced breakdown spectroscopy (LIBS) for wearable information equipment. Microsyst. Technol. **11**, 974–979 (2005). https://doi.org/10.1007/s00542-005-0508-6
32. R. Kumar, A.K. Rai, D. Alamelu, S.K. Aggarwal, Monitoring of toxic elements present in sludge of industrial waste using CF-LIBS. Environ. Monit. Assess. **185**, 171–180 (2013). https://www.ncbi.nlm.nih.gov/pubmed/22426843
33. P. Westlake, P. Siozos, A. Philippidis, C. Apostolaki, B. Derham, A. Terlixi et al., Studying pigments on painted plaster in Minoan, Roman and Early Byzantine Crete. A multi-analytical technique approach. Anal. Bioanal. Chem. **402**, 1413–1432 (2012). https://doi.org/10.1007/s00216-011-5281-z
34. W.T.Y. Mohamed, Improved LIBS limit of detection of Be, Mg, Si, Mn, Fe and Cu in aluminum alloy samples using a portable Echelle spectrometer with ICCD camera. Opt. Laser Technol. **40**(1), 30–38 (2008). https://www.sciencedirect.com/science/article/pii/S0030399207000643
35. L. Burgio, K. Melessanaki, M. Doulgeridis, R. Clark, D. Anglos, Pigment identification in paintings employing laser induced breakdown spectroscopy and Raman microscopy. Spectrochim. Acta Part B Atom. Spectrosc. **56**(6), 905–913 (2001). https://

www.sciencedirect.com/science/article/abs/pii/S0584854701002154
36. N. Rajagopalan, A.S. Khanna, Effect of size and morphology on UV-blocking property of nanoZnO in epoxy coating. Int. J. Sci. Res. Publ. **3**(4), 1–14 (2013). https://pdfs.semanticscholar.org/6d46/d50a8a42507d5c25ce01b92fe032fa1c1908.pdf
37. Can A, Sivrikaya H. *Effects of Nano-Zinc Oxide Based Paint on Weathering Performance of Coated Wood. Proceedings of the 3rd International Conference on Processing Technologies for the Forest and Bio-based Products Industries (PTF BPI 2014) Kuchl/Salzburg*, *Austria*, September 24–26, 2014, p. 1–7. http://akademikpersonel.bartin.edu.tr/acan/bildiri/acan16.09.2014_16.12.17bildiri.pdf
38. R.L. Feller, M. Wilt, Evaluation of Cellulose Ethers for Conservation, Research in Conservation, The J. Paul Getty Trust, 1990. https://www.getty.edu/conservation/publications_resources/pdf_publications/pdf/ethers.pdf
39. V. Horie, *Materials for Conservation: Organic Consolidants, Adhesives and Coatings*, 2nd edn. (Butterworth-Heinemann, Oxford, 2010)
40. O.M. El-Feky, E.A. Hassan, S.M. Fadel, M.L. Hassan, Use of ZnO nanoparticles for protecting oil paintings on paper support against dirt, fungal attack, and UV aging. J. Cult. Herit. **15**(2), 165–172 (2014). https://www.sciencedirect.com/science/article/abs/pii/S1296207413000642
41. M.S. Ghamsari, S. Alamdari, W. Han, H. Park, Impact of nanostructured thin ZnO film in ultraviolet protection. Int. J. Nanomed. **12**, 207–216 (2017). https://www.ncbi.nlm.nih.gov/pmc/articles/PMC5216680/pdf/ijn-12-207.pdf
42. M.P. Mateo, T. Ctvrtnickova, G. Nicolas, Characterization of pigments used in painting by means of laser-induced plasma and attenuated total reflectance FTIR spectroscopy. Appl. Surf. Sci. **255**(10), 5172–5176 (2009)
43. F.S.L. Borba, J. Cortez, V.K. Asfora, C. Pasquini, M.F. Pimentel, A.M. Pessis, H.J. Khoury, Multivariate treatment of LIBS data of prehistoric paintings. J. Braz. Chem. Soc. **23**(5), 958–965 (2012)
44. N. Thomas, B. Ehlmann, D. Anderson, S.M. Clegg, O. Forni, S. Schröder et al., Characterization of hydrogen in basaltic materials with laser-induced breakdown spectroscopy (LIBS) for application to MSL ChemCam data. J. Geophys. Res. Planets **123**, 1996–2021 (2018). https://doi.org/10.1029/2017JE005467